

Generic Type 3 WT models: comparison between IEC and WECC approaches

ISSN 1752-1416
 Received on 5th November 2018
 Revised 15th January 2019
 Accepted on 6th February 2019
 doi: 10.1049/iet-rpg.2018.6098
 www.ietdl.org

Alberto Lorenzo-Bonache¹ ✉, Andres Honrubia-Escribano¹, Jens Fortmann², Emilio Gómez-Lázaro¹

¹Wind Energy and Power Systems Department, Renewable Energy Research Institute, Universidad de Castilla-La Mancha, Albacete, Spain

²HTW Berlin-University of Applied Sciences, Berlin, Germany

✉ E-mail: alberto.lorenzo@uclm.es

Abstract: The widespread use of renewable energies around the world has generated the need for new tools and resources to allow them to be properly integrated into current power systems. Power system operators need new dynamic generic models of wind turbines and wind farms adaptable to any vendor topology and which permit transient stability analysis of their networks with the required accuracy. Under this framework, the International Electrotechnical Commission (IEC) and the Western Electricity Coordinating Council (WECC) have developed their own generic dynamic models of wind turbines for stability analysis. Although these entities work in conjunction, the focus of each is slightly different. The WECC models attempt to minimise the complexity and number of parameters needed, while the IEC approach aims to optimise comparison with real turbine measurements. This study presents a detailed comparison between these two different approaches for modeling a Type 3 (i.e., DFIG) wind turbine in MATLAB/Simulink. Finally, several simulations are conducted, with which the consequences of the different approaches are evaluated. The results of this paper are of interest to power system operators as well as wind turbine manufacturers who require further assistance in adapting their specific models to the simplified versions provided by the International Committees.

Nomenclature

| | |
|----------------|-----------------------------|
| P control | active power control |
| Q control | reactive power control |
| Q limitation | reactive current limitation |

1 Introduction

The current needs of power systems around the world have resulted in the development of new tools and resources that permit the integration of the increasingly important renewable energy sources. Power system operators such as transmission system operators (TSOs) or distribution system operators (DSOs) need to perform transient stability analysis in order to react to dynamic grid events such as voltage dips, loss of loads or generation, and switching of lines [1]. However, there is a lack of universal, standardised, publicly available and validated wind turbine (WT) models that allow these analyses to be conducted. For example, conventional vendor models only represent one specific WT model. Furthermore, since vendor models are intended to simulate the behaviour of specific components and controls of the WT [2, 3], they are complex, and require many parameters and specific simulation software [4].

To meet the needs of TSOs and DSOs, international organisations such as the International Electrotechnical Commission (IEC) and the Western Electricity Coordinating Council (WECC) have been working in recent years on the development of generic WT and wind farm models for power system stability analysis [5, 6]. These generic models can represent the behaviour of any vendor's WT model. Their aim is to provide sufficiently accurate results without the need for a large number of parameters, and with sufficient documentation for them to be implemented in any simulation software. In February 2015, the IEC published the first edition of the Standard IEC 61400-27-1 [7]. The second edition of this standard is currently under development, and is expected to be published in 2019. In January 2014, the WECC published their report entitled 'WECC Second Generation Wind Turbine Models' [8], the first generation of which was published in 2010 [9]. These two documents classify the different topologies of WTs into four types [10], depending mainly on their

electrical generator. Type 3, which is studied in this paper, represents a WT equipped with a doubly fed induction generator (DFIG)/asynchronous generator, in which the stator is directly connected to the grid and the rotor is connected through an alternating current (AC)/direct current (DC)/AC power converter [11]. Worldwide, this is the most commonly installed topology of WT [12]. In addition, the Type 3 simulation model is the most complex of the four types for both International Committees.

WT manufacturers are the most important stakeholders involved in the development of these generic models, providing field data and values of the parameters that define their behaviour. The first generation WECC models were developed primarily by one manufacturer, while development of the second generation coincided with that of the IEC, with the involvement of manufacturers such as GE, Siemens, ABB, REpower/Senvion, and to a limited extent Vestas and Gamesa, who contributed to both models. The IEC model was later extended, based mainly on data provided by Gamesa, Senvion, and Vestas. The debate on IEC and WECC models is based primarily on issues of complexity (number of states), number of parameters and model execution speed (in the focus of WECC [13]), and accuracy during faults close to 90% voltage, as well as unbalanced conditions, in order to fulfil the validation requirements in certain European countries, which is the IEC's main goal. Hence, the comparison of the response provided by both models plays a key role in spreading their use and application in current power systems.

With reference to the existing literature, a number of implementation and validation works regarding IEC and WECC generic models have been published. One of the first published works on generic WT models is [14], which shows the development of the WECC models (the first version of the WECC's guidelines was published in 2010). Concerning the IEC standard, which was published subsequently (2015), the first works focused on modelling can be found in [15–17], which also describe the ongoing work. Furthermore, in 2011 Asmine *et al.* [18] and Keung *et al.* [19] started to investigate validation methodologies for generic WT models. During the following years, contributions focused on the development of the second generation of WECC WT models [20–22], as well as the first edition of the IEC 61400-27-1 [23–25]. Since the publication of the standard, the

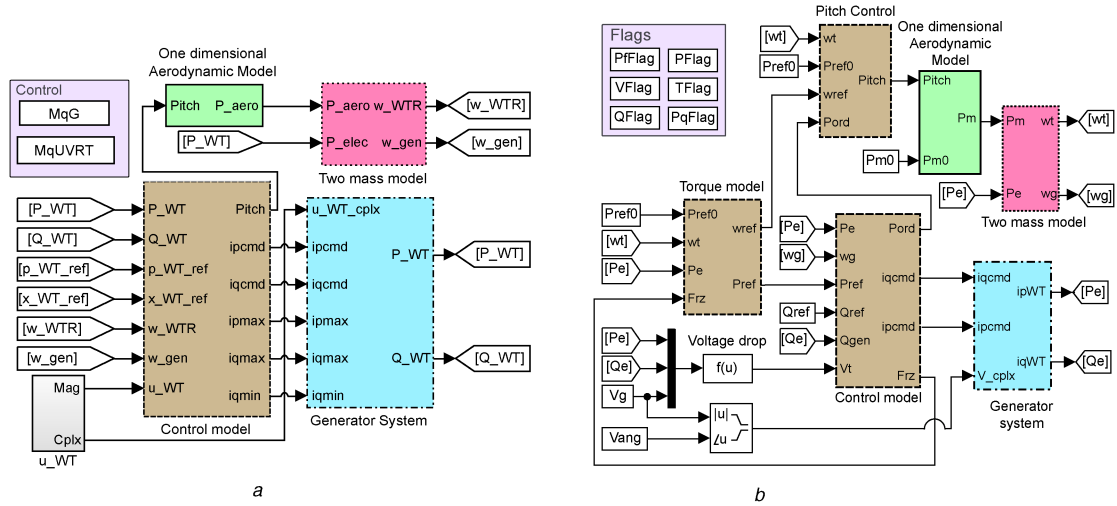


Fig. 1 General structure of the generic Type 3 models defined by both international guidelines
(a) IEC 61400-27-1 Simulink implementation, (b) WECC Simulink implementation

modelling of IEC generic WT models has been widely studied [26–28], with other works also addressing the second generation WECC models [29]. Furthermore, validation efforts have been conducted since the publication of IEC 61400-27-1 and WECC second generation models. In this sense, one of the first validation works corresponds to [30], in which a generic Type 3 WECC model is validated, considering first and second generations, as well as a manufacturer model. In [31], the IEC validation methodology is presented and implemented on both an IEC Type 3 generic model and a manufacturer model. Later, the validation of an IEC Type 3 generic WT model with field data is conducted in [32]. Finally, Lorenzo-Bonache *et al.* [33] show the field validation of generic Type 4 WT models, both IEC and WECC. Other validation works regarding generic models have been conducted such as [34, 35], in which field validation of wind farm models is conducted with IEC and WECC guidelines, respectively. These previous contributions demonstrate that generic WT models may accurately represent the behaviour of real WTs. Nevertheless, only limited detailed information is publicly available for a detailed comparison between the models described by these two references [36].

IEC and WECC generic simulation models share many systems and characteristics, which can be implemented equally for both models. Other features differ from one document to the other. This work aims to provide a better understanding of the differences between the two implementations of generic models, as well as emphasising the consequences of the different perspectives of each international guideline. The point of departure is a generic Type 3 WT model based on the IEC 61400-27-1 guidelines [7], modelled in MATLAB/Simulink, which has been validated with field data in previous works by Lorenzo-Bonache *et al.* [27], Honrubia-Escribano *et al.* [31], and Lorenzo-Bonache *et al.* [37]. The generic Type 3 model based on the WECC guidelines [8] was also implemented in MATLAB/Simulink. The differences between these two modelling approaches were studied in detail. It is important to note that the models described in WECC are usually linked to a predefined model of specific software such as GE PSLFTM and Siemens PTI PSS[®]E, and hence their implementation in MATLAB/Simulink involves several possible interpretations, because not every detail of the implementation is fully described in the document [38]. This is a major advantage for the IEC models, which are described regardless of the simulation software. Finally, different tests were conducted to evaluate the additional features provided by the IEC model, as well as the advantages of simplicity of the WECC model. Regarding the parameterisation of the models, the authors defined the specific values in the previously cited works [27, 31, 37]. On the basis of these, the values and ranges of the current work are not intended to represent a specific WT commercial model, but to provide logical and tested scenarios, in which the models may perform properly, as well as showing their differences.

The contributions of the present study focus on: (i) providing guidelines on the adjustment of a generic Type 3 WT model based on the two international guidelines related to this topic (IEC 61400-27-1 Ed. 1 and WECC second generation of WT models); (ii) conducting an in-depth analysis regarding the consequences of the different points of view of each entity; and (iii) testing the compatibility between the two implementation approaches. Hence, this paper can be of particular interest not only for researchers working on the development of generic models, but also for manufacturers intending to adjust their particular models to either of these two references, as well as for power system operators (TSOs and DSOs). Finally, these results support the IEC and WECC Committees, as a reference to check the compatibility between the models, as well as the advantages of each entity approach.

This paper is structured as follows: after this introduction, Section 2 gives an overview of the generic Type 3 models based on the guidelines provided by both committees. Section 3 examines the systems which differ most between the two documents. Section 4 describes the results of testing the compatibility of both models, depicting the consequences of the two perspectives: accuracy or simplicity. Section 5 presents the conclusions of this work.

2 Generic Type 3 WT model

Fig. 1a shows the general structure of the generic Type 3 WT model described in IEC 61400-27-1 [7], which has been modelled in MATLAB/Simulink. The systems included in the control model, which can be seen in the centre of Fig. 1a (brown colour), are: *active power control* (P control), *reactive power control* (Q control), *pitch control*, *current limitation system* (CLS), and *reactive power limitation* (Q limitation). It also includes two reference values of active and reactive powers (p_{WT_ref} and x_{WT_ref} , respectively), as well as two control parameters, which command the reactive power control mode and the behaviour when the WT is submitted to a voltage dip (MqG and MqUVRT, respectively). Finally, the definition of the voltage profile is performed according to the definition of its magnitude and its phase (left-hand side of Fig. 1a – subsystem u_{WT} provides the magnitude and the complex signal).

Fig. 1b shows the general block diagram of the generic Type 3 model implemented in MATLAB/Simulink following WECC guidelines [8]. In this case, the active and reactive power references are referred to as Pref0 and Qref, respectively. Flags PFlag, VFlag, and QFlag, which can be seen on the left-hand side of Fig. 1b, play the same role as MqG in the IEC model. PqFlag corresponds to the parameter Mqpri included in the CLS of the IEC model. Finally, parameters PFlag and TFlag do not correspond to any parameter in the IEC model, because the modes they set are predefined in the IEC model, as will be explained later in Section 3. In the WECC, WT model, the P control, the Q control and the

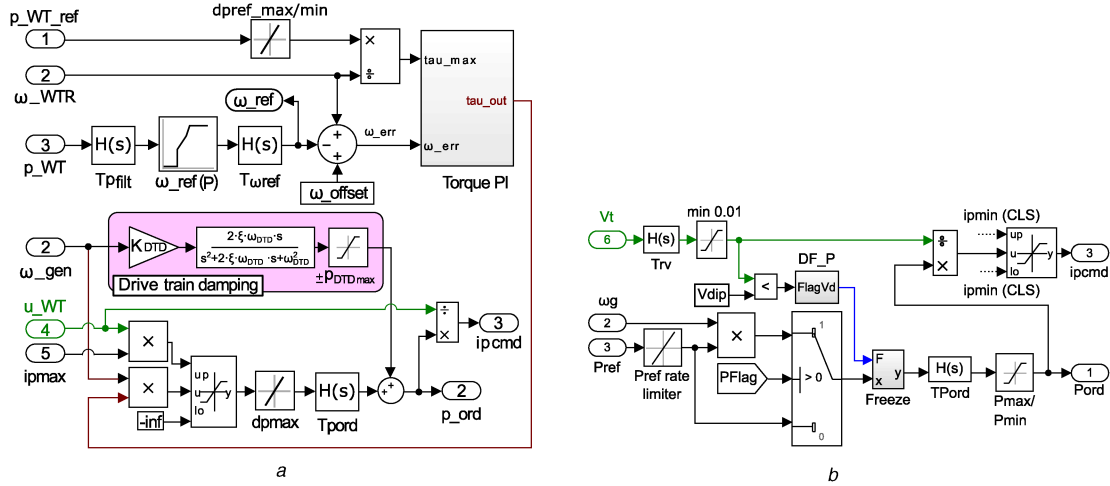


Fig. 2 Simulink implementation of the Type 3 active power control defined by both international guidelines (a) IEC 61400-27-1, (b) WECC second generation

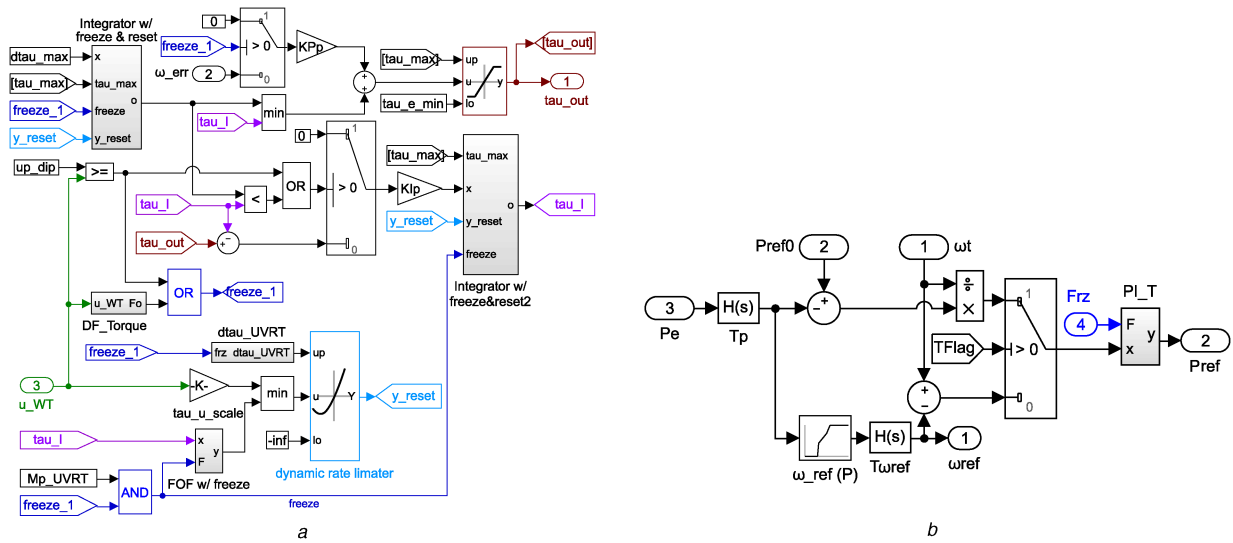


Fig. 3 Simulink implementation of the Type 3 torque PI subsystem defined by both international guidelines (a) IEC 61400-27-1, (b) WECC second generation

CLS systems are included in the control model [29], without subsystem separation, contrary to the IEC model. However, in this work they will be separated in order to facilitate the understanding of the differences between both modelling approaches.

As members of both international working groups have collaborated almost since their inception, some systems have been implemented in the same form for both generic WT models [39]. These systems are the mechanical two-mass model (pink in Fig. 1), the one-dimensional aerodynamic model (green) and the pitch control system. However, the absence of a dynamic reactive power limitation control in the WECC generic Type 3 model constitutes an important difference. In the IEC model, this system allows the reactive power limits to be controlled through look-up tables depending on the voltage or the active power at any time. The WECC model provides systems to control the reactive power, but they are set as fixed values. The remaining systems, as explained hereafter, are not equivalent for IEC and WECC generic models approaches.

3 Systems with different implementations in IEC and WECC

The following sections describe the systems with different interpretations and constructions in IEC 61400-27-1 and WECC second generation.

3.1 Active power control

The active power control systems from IEC 61400-27-1 [7] and WECC ‘Second Generation of WT models’ [8] are shown in Figs. 2a and b, respectively. Moreover, the torque proportional–integral (PI) subsystems, which are part of the active power control, despite being included in the general structure of WECC model, are shown in Figs. 3a and b, for the IEC and WECC approaches, respectively. The nomenclature followed in the diagrams corresponds to the one used by each entity. Furthermore, hereafter, the transfer function blocks indicated as $H(s)$ represent first-order filters which follow (1), in which T_{name} represents the time constant for each filter, shown in the diagrams as the name of the transfer function block.

$$H(s) = \frac{1}{sT_{name} + 1} \quad (1)$$

As can be deduced from Figs. 2 and 3, the Type 3 active power control model defined by the IEC Committee is more complex than that of the WECC. It contains more sophisticated functions for controlling power during grid faults and subsequent voltage recovery. The general behaviour of these systems is governed by the look-up table $\omega_ref(P)$ (see Figs. 2a and 3b), which provides the rotational speed at which the WT should be rotating when it is injecting a certain active power. This speed reference is subtracted from the actual rotational speed of the WT rotor (ω_WTR/ω_t) (when a parameter or signal is included in both models, but named

differently, it will be referred as $IEC_{parameter}/WECC_{parameter}$ (i.e. ω_{WTR} is the IEC parameter which refers to the rotational speed of the WT rotor, which is called ωt in the WECC guidelines), and the speed error is then the input to a PI controller, providing the electromagnetic torque of the WT (τ_{out}/P_{ref}). On the basis of Göksu *et al.* [36], the parameters of the PI controller are not the same for both models, which is explained by their different behaviour when facing a voltage dip, as explained hereafter. In the present work, they are defined as follows. Additionally, model parameters are depicted in Table 1

- $KP_p = 500/K_{pp} = 0.1$
- $KI_p = 10/K_{ip} = 0.1$

This τ_{out}/P_{ref} is then multiplied by the generator speed (ω_{gen}/ω_g) to obtain the active power of the WT (p_{ord}/P_{ord}). Finally, the active power is divided by the voltage (u_{WT}/Vt) to obtain the active current command signal ($ipcmd$), which is the input to the generator system.

The WECC model allows the selection of different control modes by flags PFlag and TFlag. PFlag establishes whether active

power control is commanded by the electromagnetic torque or the active power. Since the IEC model uses active power for this purpose, in order to obtain similar results, PFlag takes the value of 1 in this work. TFlag is included to choose between using the rotational speed error and the active power error in the torque PI system (Fig. 3b). Since the IEC model actuates according to the rotational speed error only, TFlag is equal to 0 in the present work.

The main differences between the two active power control models are related to the control during and following voltage dip, which is more complex in the IEC model. In the IEC model, the reset (freeze) system can control the torque output rate and value more accurately. When a fault occurs, the signal freeze_1 takes the value of 1, and is maintained during the fault and a certain post-fault period controlled by the delay flag block DF_Torque (Fig. 3a). The proportional component (in the upper side of Fig. 3a) then takes the value of 0. The other part of the controller takes the minimum value between two possible signals: the torque value increasing as a ramp at maximum rate $d\tau_{max}$ (which can be used either to control the mechanical stress or to meet a certain grid code) or the output of the integral part, which actuates according to the error between its own output τ_{I} and the output of the system τ_{out} . When the fault occurs, the output of the first

Table 1 Parameters associated with the generic Type 3 models, both IEC and WECC

| Symbol | Submodel | Description | Value | |
|-----------------------|---------------------|---|-------------|---------|
| | | | IEC | WECC |
| $T_{CW}(du)$ | generator | CB duration versus voltage variation | 0.05 | — |
| x_s | | electromagnetic transient reactance | [0.2 : 0.4] | — |
| | LVPL _{0.5} | LVPL gain breakpoint (V = 0.5 pu) | — | [0 : 1] |
| T_{wo} | | time constant for CB washout filter | 0.5 | — |
| dj_{pmax} | rrpwr | maximum active current ramp rate | 2.75 | — |
| M_{qG} | | reactive power control mode | 1 | — |
| | PFlag | constant Q (0) or power factor (PF) (1) local control | — | 0 |
| | Vflag | voltage control (0) or Q control (1) | — | 1 |
| | Qflag | bypass (0) or engage (1) inner voltage regulator loop | — | 1 |
| M_{qUVRT} | | under voltage ride through (UVRT) reactive power control mode | 2 | — |
| K_{qv} | kqv | voltage scaling factor for UVRT current | 0.55 | 0.60 |
| i_{qpost} | iqfrz | post-fault reactive current injection | 0.5 | — |
| r_{drop} | Rt | resistive component of voltage drop impedance | 0.01 | — |
| x_{drop} | Xt | inductive component of voltage drop impedance | 0.1 | — |
| T_{jord} | Tjord | time constant in reactive power order lag | 0.001 | — |
| u_{max} | V max | maximum voltage in voltage PI controller integral term | 1.1 | — |
| u_{min} | V min | minimum voltage in voltage PI controller integral term | 0.9 | — |
| u_{qdip} | Vdip | voltage threshold for UVRT detection in Q control | 0.9 | — |
| M_{DFSLim} | | current limitation control | 0 | — |
| M_{gpri} | | prioritisation of reactive power control during UVRT | 1 | — |
| $T_{\omega filtp3}$ | | active power control | 1 | — |
| ω_{offset} | | filter time constant for generator speed measurement | 0.0 | — |
| K_{DTD} | | gain for active DTD | [0 : 1] | — |
| T_{pfilt} | Tpt | time constant in power measurement filter | 0.001 | — |
| T_{pord} | Tpord | time constant in power order lag | 0.001 | — |
| T_{ufilt} | Tuord | time constant in voltage measurement filter | 0.001 | — |
| dp_{max} | dprefmax | maximum WT power ramp rate | 1 | — |
| T_{oref} | twref | time constant in speed reference filter | 200 | — |
| $d_{\tau_{au, UVRT}}$ | | torque PI | [0 : 1] | — |
| $\tau_{au_u_scale}$ | | limitation of torque rise rate during UVRT | [0 : 1] | — |
| KPp | Kpp | voltage scaling factor of reset torque | 500 | 0.1 |
| KIp | kip | proportional constant of torque PI controller | 10 | 0.1 |
| Kpx | Kcc | integral constant of torque PI controller | [0 : 0.04] | 0.016 |
| Θ_{max} | Θ_{max} | pitch cross-coupling gain | 30 | — |
| Θ_{min} | Θ_{min} | maximum pitch angle | 0 | — |
| $d\Theta_{max}$ | $d\Theta_{max}$ | minimum pitch angle | [5 : 10] | — |
| $d\Theta_{min}$ | $d\Theta_{min}$ | maximum pitch angle rate | [-10 : -5] | — |
| | | minimum pitch angle rate | | |

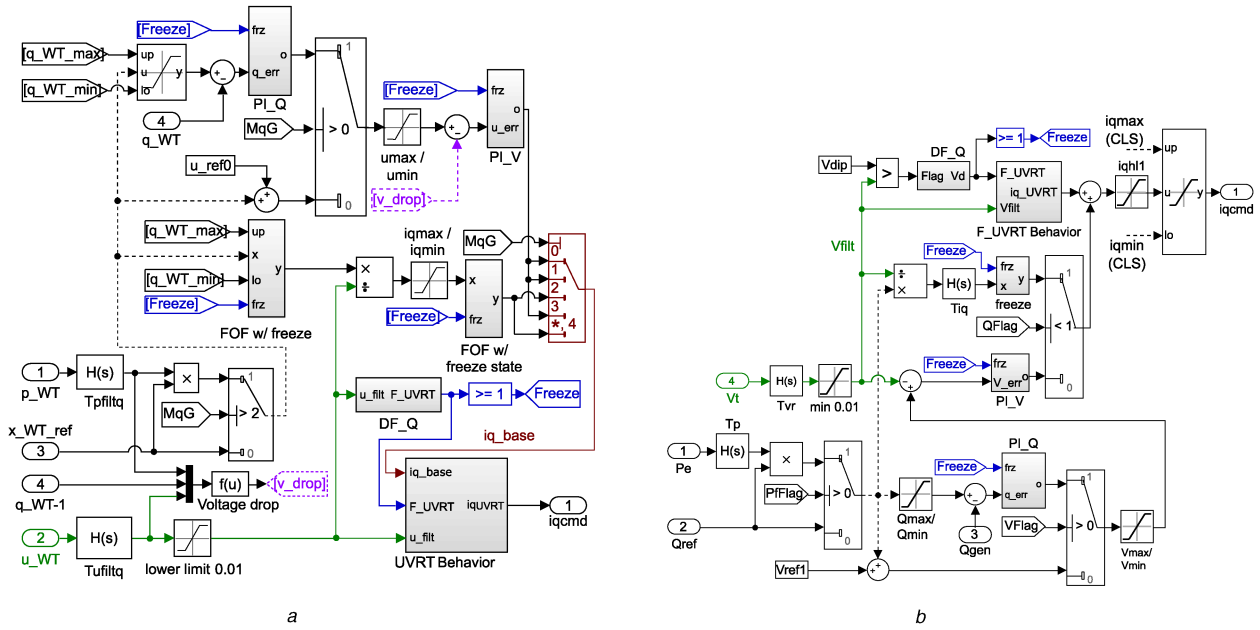


Fig. 4 Simulink implementation of the Type 3 Reactive power control defined by both international guidelines
(a) IEC 61400-27-1, (b) WECC second generation

Table 2 Correspondence between control flags for reactive power control

| IEC MqG | WECC | | | Control mode |
|---------|--------|-------|-------|----------------------------------|
| | PfFlag | VFlag | QFlag | |
| 0 | 0 | 0 | 1 | voltage control |
| 1 | 0 | 1 | 1 | reactive power control |
| 2 | 0 | 1 | 0 | open-loop reactive power control |
| 3 | 1 | 1 | 1 | power factor control |
| 4 | 1 | 0 | 0 | open-loop power factor control |

system takes the value y_{reset} , and the second can either continue working according to its input or be forced to value y_{reset} , depending on the parameter Mp_{UVRT} . This value y_{reset} is calculated as the minimum between the residual voltage multiplied by the gain τ_{u_scale} or the value τ_{u_I} . The maximum rate of y_{reset} is also modified during the dip (system $d\tau_{UVRT}$), usually not allowing y_{reset} to increase during the fault. After the post-fault period, the proportional component continues working according to ω_{err} , and the integral part will increase from y_{reset} to the steady-state value, with a maximum rate defined by $d\tau_{u_max}$.

The WECC torque control system is defined as a PI controller working either with the torque or the rotational speed error, depending on $TFlag$, as previously explained. During the fault, the PI controller is frozen, which means that the proportional part takes the value of 0, as well as the input to the integral part (keeping constant its output). This behaviour constitutes a key difference to the IEC model. The WECC system maintains the steady-state value during the fault, while the IEC approach is able to adjust it by use of the parameters τ_{u_scale} and $d\tau_{UVRT}$. Thus, for the WECC model, the value of the active power during the fault depends only on the dip depth, and its control or adjustment is not possible. The consequences of this different behaviour are discussed in-depth in Section 4.

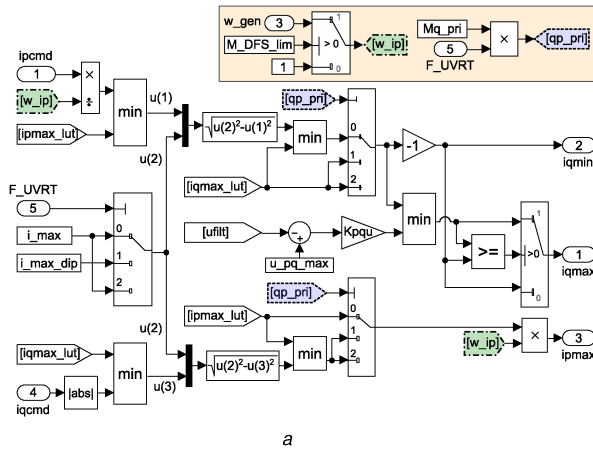
3.2 Reactive power control

The Simulink implementations of the Type 3 reactive power control systems from IEC and WECC are shown in Figs. 4a and b, respectively. Both systems work similarly, using flags to define the path the reference signal must follow. In both cases, the reactive power reference is assumed to come from a plant controller. It can be either a reactive power reference or a voltage reference. A number of switches allow the activation of different control types. In the IEC model, a single flag (MqG , whose value is between 0

and 4) is used, while three flags are needed in the WECC model ($PfFlag$, $VFlag$, and $QFlag$, which can be defined as 0 or 1) [40]. The correspondence between the flags is shown in Table 2, where it can be observed that the same control modes are available. Open-loop controls ($MqG = 2$ and 4) can only be used if the power plant controller is built, which is not the case of this work.

The control mode chosen for the simulations is a closed-loop reactive power control, following the reference x_{WT_ref}/Q_{ref} . The reference signal goes through two PI controllers: one actuating according to the reactive power error and other actuating according to the voltage error. Then, the reactive current command signal (iq_{cmd}), which is the input to the electrical generator system, is obtained.

In terms of the behaviour of the system under a voltage dip, the IEC model is more complex, as it allows a choice between three control modes. For the IEC model, three different control modes can be chosen by adjusting the parameter Mq_{UVRT} . If Mq_{UVRT} takes the value of 0, the reactive current injected during the dip is proportional to the voltage depth; when Mq_{UVRT} is set to 1, the reactive current injected during the dip depends on the current injected prior to the fault plus a value proportional to the voltage depth; finally, if Mq_{UVRT} takes the value of 2, the behaviour is the same as Mq_{UVRT} equal to 1, but adding a constant reactive current component during a certain post-fault period. The WECC model, the transient control system of which is included in the block F_{UVRT} Behavior, directly implements the most complex system. Hence, the WECC transient control system is modelled as the IEC one with Mq_{UVRT} equal to 2. Thus, the behaviour of Mq_{UVRT} can be obtained if $iq_{post} = 0$. However, the mode Mq_{UVRT} equal to 0 is not equivalent between both systems, since the current from the steady-state controller is always added in the WECC model. Furthermore, another difference is that the IEC model uses the steady-state voltage to obtain the depth of the dip (adjusting the time constant of a first-order filter with a large value,



```

%% MATLAB code for CLS
if Pqflag==0 %Q priority
    iqmax=min(VDL1, I_max)
    ipmax=min(VDL2, sqrt(I_max^2-iqcmd^2))
else %P priority
    iqmax=min(VDL1, sqrt(I_max^2-iqcmd^2))
    ipmax=min(VDL2, I_max)
end
iqmin=-iqmax
ipmin=0

```

Fig. 5 Implementation of the Type 3 CLSs defined by both international guidelines (a) IEC 61400-27-1 Simulink implementation, (b) WECC second generation MATLAB code

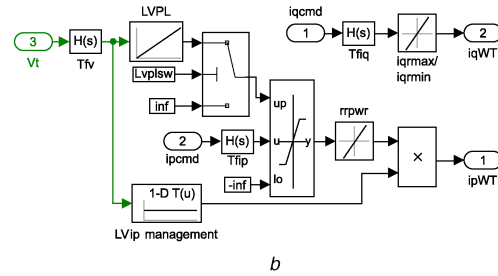
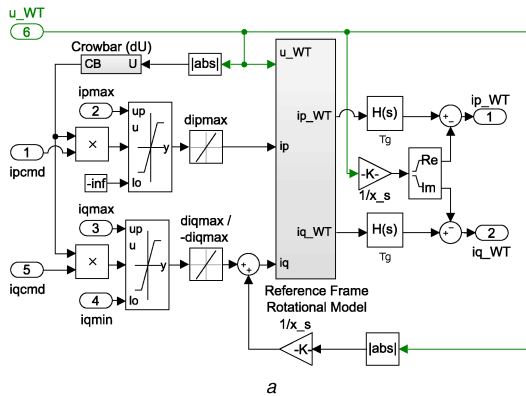


Fig. 6 Simulink implementation of the Type 3 generator systems defined by both international guidelines (a) IEC 61400-27-1, (b) WECC second generation

e.g. 100 s), while the WECC model uses a predefined value (V_{ref0}).

Another important difference regarding the reactive power control system, which also affects the behaviour of active power and CLSs, is that the IEC model uses the voltage profile defined as the input to the system (u_{WT}) in order to calculate, for example, the reactive power injected during the voltage dip. In contrast, the WECC model uses the voltage in the high-voltage (HV) terminal of the transformer (V_t) to conduct these operations. This voltage V_t is calculated as the voltage in a point which is located using the serial impedance from the WT terminal (typically a transformer). This means that, during the dip, due to the reactive power injection and low active power consumption, $V_t > u_{WT}$, and hence, parameters such as K_{qv} (used to calculate the reactive power proportional to the dip depth that should be injected during the fault) have to be adjusted using different values in both models to obtain the same response. For the current work

- $K_{qv, IEC} = 0.55$ pu.
- $K_{qv, WECC} = 0.60$ pu.

Finally, as commented in Section 1, the IEC model implements a dynamic reactive power limitation system. The signals q_{WT_max} and q_{WT_min} , which can be seen in Fig. 4a, are obtained from this limitation system. Both signals are calculated by use of the minimum value between two look-up tables, dependent on the u_{WT}/V_t and the active power provided P_{WT}/P_e . The WECC model uses static limiters, as shown in Fig. 4b.

3.3 Current limitation system

The Simulink implementation of the Type 3 CLS from IEC 61400-27-1 is shown in Fig. 5a, while the logic followed by the WECC guideline is depicted in the MATLAB code shown in

Fig. 5b. The behaviour of both systems regarding the maximum current which can be provided by the WT follows the logic defined in the WECC report [8], shown in Fig. 5b. In the IEC system, parameter Mq_pri is equivalent to flag $PqFlag$, which is used for selecting active or reactive current priority. However, in the IEC model, this priority is only set during faults (Mq_pri is multiplied by F_{UVRT}), while in steady state the priority is always set to active power.

During faults, the IEC system allows modification of the maximum current which can be injected by the WT, using the definition of the parameter i_{max_dip} (during a fault, the maximum current is usually smaller). Moreover, by using parameter M_DFS_lim (found in the highlighted square of Fig. 5a), this model allows the maximum active current ip_{max} to be multiplied by the rotational speed of the generator ω_{gen} , which is equivalent to limiting the total current ($M_DFS_lim = 0$) or the stator current ($M_DFS_lim = 1$). Finally, the maximum reactive current can also be defined by the partial derivative of reactive current limit versus voltage $Kpqu$ (i.e. the IEC model allows the maximum reactive current to be controlled depending on the voltage level). These three considerations are not included in the WECC model, and thus, the control of the current injected during the fault can be more accurately adjusted in the IEC model, despite the larger number of parameters used. There can also exist differences because of the use of u_{WT} or V_t as input of the look-up tables, as previously commented in Section 3.2.

3.4 Type 3 generator system

The Simulink implementation of the Type 3 generator systems from IEC and WECC is shown in Figs. 6a and b, respectively. The WECC generator system is a simplification of the IEC system, which is based on [24, 41]. In the WECC approach, the current command signals are only filtered and saturated. However, after

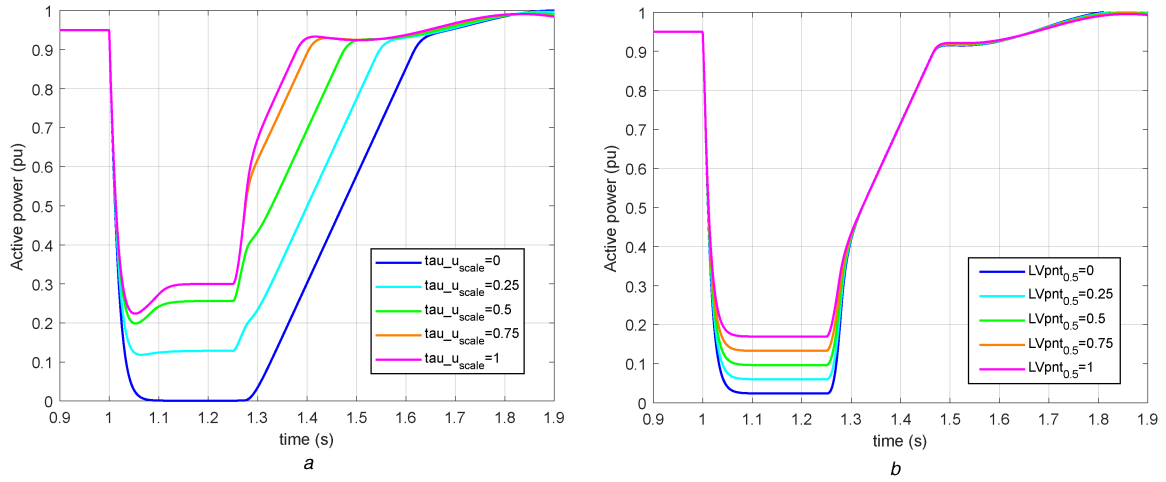


Fig. 7 Active power response during a fault
(a) IEC 61400-27-1 Type 3: τ_{u_scale} variation, (b) WECC Type 3: LV_{pnt} variation

these operations in the IEC approach, the voltage terminals are coordinated to the grid (*reference frame rotational model*), and the dynamics of the generator reactance are considered (x_s) [37], describing the impact of the rotor flux derivative. The addition of this component allows a better control of the transient behaviour when the fault occurs. Moreover, the IEC generator system considers the crowbar (CB) protection system, which is a conventional technology used to avoid the disconnection of the WT during the voltage dip [26, 42]. This system actuates when the variation of the voltage is larger than a threshold, and multiplies by 0 the currents over a certain period of time.

The WECC generator system includes transient control systems such as a *low-voltage (LV) active current management*, which has been modelled as a look-up table (*LVip management* in Fig. 6b) or the *LV power logic* (LVPL) system, conventionally used by WTs during faults. Furthermore, the WECC generator system also features HV reactive current management, but since no HV case is considered in this work, it is not included here. These managing systems are detailed in [43]. Finally, the active and the reactive powers injected to the grid are calculated as usual, using the equation below:

$$P_{WT} + jQ_{WT} = (ip_{WT} + j \times iq_{WT})|u|_{WT} \quad (2)$$

It is important to emphasise that the reactive power should be considered with capacitive sign convention, and all the systems are modelled following this reference. Reactive currents and reactive power have the same sign convention. It is considered that the reactive current follows the equation below::

$$iq_{WT} = -\text{Im}(\bar{i}_{WT}) \quad (3)$$

4 Generic Type 3 simulation results

Simulations were carried out in order to identify the different features that both generic model approaches offer. First, the differences in the active power response are analysed, which are mainly due to the differences in the control approaches described in Section 3.1. Furthermore, the consequences of the different perspectives in the response of the pitch angle are analysed, as well as the action of the CB protection system. Then, the influences of the different implementations of the electrical generator system are studied for the reactive power behaviour. Finally, the benefits of the WECC perspective regarding simplicity are studied.

4.1 Active power response

First, the consequences of the different torque control behaviours during the fault are shown in Fig. 7. The simulation carried out consisted of a voltage dip with a residual voltage of 0.5 pu and a duration of 200 ms. For the IEC model (Fig. 7a), the active power value during the voltage dip depends on the voltage depth and the

parameter τ_{u_scale} , as described in Section 3.1. Depending on the value of τ_{u_scale} , the output of torque PI system (Fig. 3a) during the fault is calculated. For the cases, in which $\tau_{u_scale} = \{0; 0.25; 0.5\}$, the active power is limited by torque PI system, whereas for the cases $\tau_{u_scale} = \{0.75; 1\}$ the active power is limited by the CLS. For these last two cases, it can be seen that the value of τ_{u_scale} modifies the value from which the active power recovers its steady-state value at nominal rate. The time at which this occurs is the same for all cases, but since the value from which the recovery begins is different, the time needed to reach the steady state varies. The active power control system of the WECC model contains no system that can control the value of torque during the fault (Fig. 7b). Moreover, the torque value during the fault is frozen, and thus does not decrease as for the IEC model. The only way provided by the WECC guidelines to modify the value during the fault is the *LV active current management* system included in the *generator system* (Fig. 6b). However, as shown in Fig. 7b, this system does not provide such complete control as the IEC model, since it only modifies the active power value during the fault, but the recovery is equal for all cases.

Additionally, this electromagnetic torque control involves a different behaviour in the *pitch control* system, shown in Fig. 8. The *pitch control* model is depicted in detail in [27]. It is composed of two PI controllers, which depend on the rotational speed error (ϵ_ω – between ω_{WTR}/ω_t and ω_{ref}) and the active power error (ϵ_c – between p_{ord}/P_{ord} and $p_{WT,ref}/Pref0$). However, both guidelines consider the possibility of using a cross-coupling gain K_{PX}/K_{cc} , which is used to add the active power error to the rotational speed error, and hence uses only one PI controller, which is the case considered in this work. In this sense, the use of only one PI controller avoids certain coordination issues. The difference in the behaviour of the torque controller in both guidelines has an influence on ϵ_c . The signals p_{ord}/P_{ord} , as shown in Fig. 2, are directly calculated by multiplying the torque by the rotational speed of the generator. Hence, for the IEC model, p_{ord} decreases to a value dependent on τ_{u_scale} , whereas P_{ord} (WECC approach) is maintained constant (except for the oscillations after the fault). Then, for the IEC model, ϵ_c is negative during the fault, which causes a decrease in pitch angle. Under the assumption that the WT is working at partial load (i.e. pitch angle is 0°, which means that the electric power is equal to the wind power absorbed by the blades), what is obtained is a delay in the time at which the pitch angle starts to increase. This is shown in Fig. 8a. The simulation conducted consisted of a voltage dip with a residual voltage of 0.5 pu and a duration of 500 ms. The delay can be controlled by adjusting K_{PX} , which controls the proportion of ϵ_c in the input error to the pitch PI controller. This variation of pitch angle has an important influence in the rotational speed of the WT, which needs

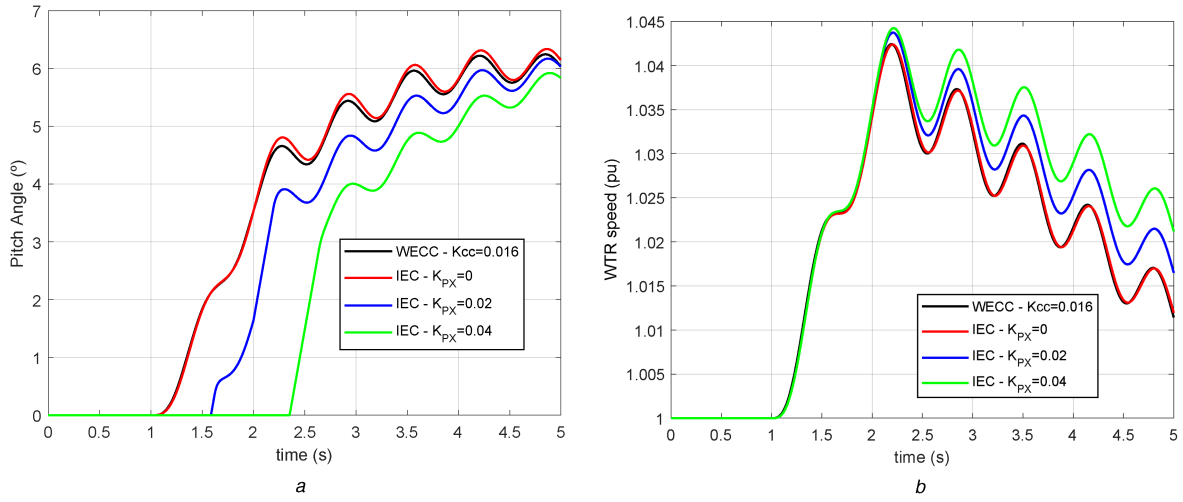


Fig. 8 Influence of torque control implementation in the pitch angle and rotor speed
 (a) Modification of pitch response due to torque control, (b) Influence of pitch variation in rotor speed

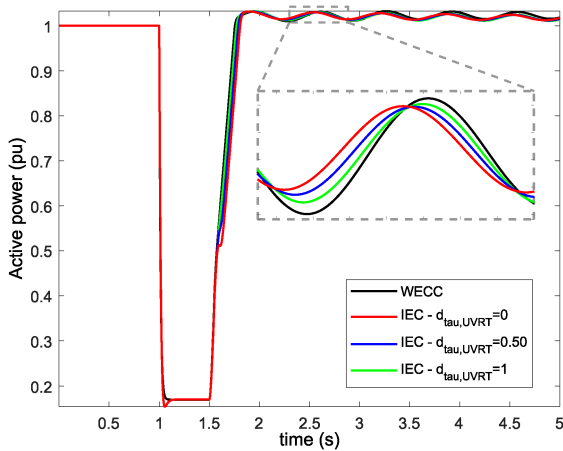


Fig. 9 Voltage post-fault control ($Mp_UVRT = 1$) varying $d_{\tau,UVRT}$

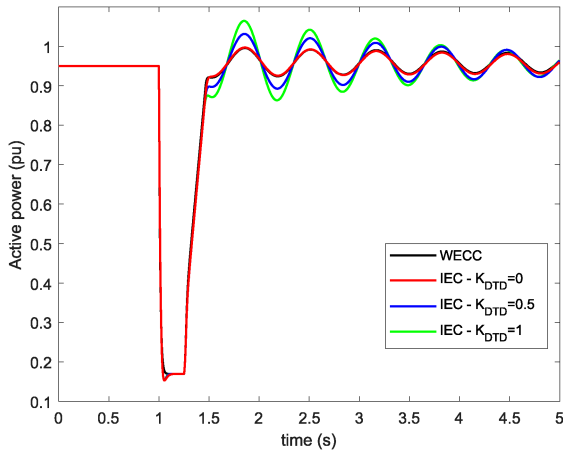


Fig. 10 Control of oscillations by the active DTD system

more time to recover the steady-state condition, as shown in Fig. 8b.

Regarding the control of the active power during the post-fault period, Fig. 9 shows the voltage post-fault control mode provided by the IEC model by adjusting the parameter $Mp_UVRT = 1$. This control mode freezes the output of torque PI control system for a certain time T_{DVS} , set to 0.1 s for this study. During this time, the output of torque PI system takes the value y_reset (Fig. 3a). When the fault is cleared, u_{WT} recovers the value 1 pu, and thus, the value of y_reset tends to increase. During T_{DVS} , this rise will depend on the maximum rate defined by the parameter $d_{\tau,UVRT}$. As shown in Fig. 9, the adjustment of this parameter allows the active power

behaviour to be controlled after the fault. Furthermore, as shown in the zoom included in Fig. 9, with the variation of this parameter, the mechanical oscillations phase can be modified. The frequency of these oscillations is calculated according to (4) [7]. From the value $d_{\tau,UVRT} = 0$ to $d_{\tau,UVRT} = 1$, the phase is modified by 28.45° . WECC system (black colour in Fig. 9) does not provide any similar post-fault control mode, and the active power increases at a constant ramp rate. As $d_{\tau,UVRT}$ increases, the behaviour of the IEC model approximates to that of the WECC

$$\omega_{osc} = \sqrt{k_{drt} \times \left(\frac{1}{2H_{WTR}} + \frac{1}{2H_{gen}} \right)} \quad (4)$$

$$= \sqrt{237.7854 \text{ pu} \left(\frac{1}{2 \times 10 \text{ s}} + \frac{1}{2 \times 1.5 \text{ s}} \right)} = 9.5473 \text{ rad/s}$$

Moreover, not only can the oscillation phase be more accurately adjusted by the IEC model, but also its magnitude. For the WECC approach, this behaviour depends only on the dynamics of the two-mass model. However, as explained in Section 3, the *active power control* of the IEC model includes the active drive train damping (DTD) system, which is able to control the amplitude, as shown in Fig. 10 (the black signal – WECC – coincides with the red one – IEC $K_{DTD} = 0$). As a consequence, due to the capability of controlling the phase and the magnitude of the mechanical oscillations during the post-fault period, the IEC model presents further options of flexibility and adaptability.

Finally, Fig. 11 shows the influence of the CB system included in the IEC electrical generator system. The WECC curve coincides with that of the IEC without CB. Since the operation of the CB system consists of multiplying the active current commanded by the control system (ip_{cmd}) by zero, the active power consequently decreases. The CB system depends on the variation of the voltage, defining the time which is activated by adjusting the positive and negative thresholds (i.e. it is possible to define if it only actuates when the fault occurs and/or is cleared, as well as for how long it is activated). From Fig. 11, it can also be observed that the oscillation phase is also modified by the CB system.

4.2 Reactive power response

Since both (IEC and WECC) reactive power control systems are similar, and the control mode after the fault is defined in the same way, the differences related to reactive power response are mainly due to the electrical generator system.

First, the influence of including the dynamics of the electrical generator reactance (x_s in Fig. 6a) on the reactive power response is studied (Fig. 12). For all the simulation cases conducted in this section, the voltage dip was defined with a depth of 0.5 pu and a duration of 500 ms, and the CB system is deactivated. Moreover, the voltage angle is kept as 0 during the simulation (i.e.

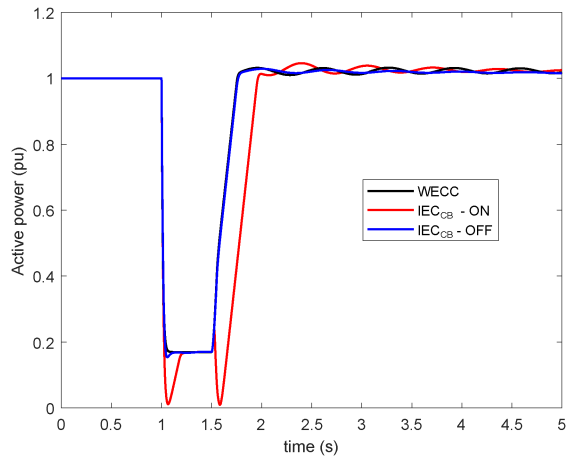


Fig. 11 Influence of the CB system in the active power response

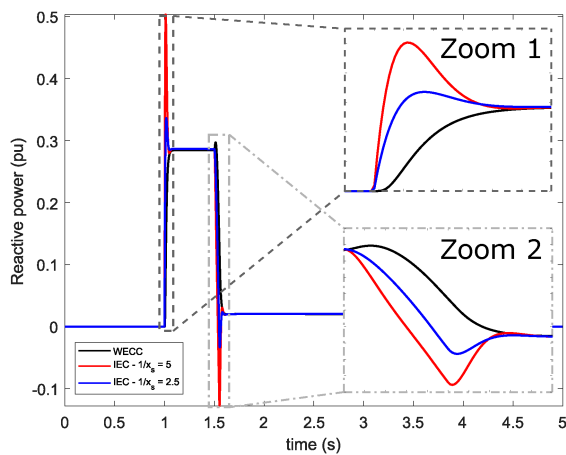


Fig. 12 Influence of the parameter x_s on the reactive power response

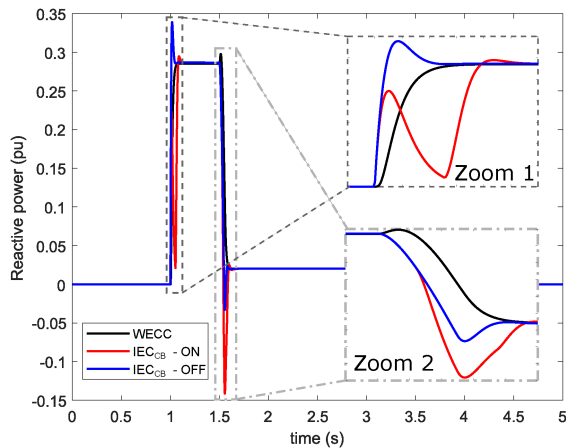


Fig. 13 Influence of the CB system on the reactive power response

$\text{abs}(u_{WT}) = \text{Re}(u_{WT})$). As shown in Fig. 6a, both these magnitudes are multiplied by $1/x_s$ and then added before and after the filter which models the dynamics of the converter. This causes a delay between the two additions, causing the peaks shown in Fig. 12, which are zoomed before and after the fault (Zoom 1 and Zoom 2). The values $x_s = \{0.2, 0.4\}$ are representative of real values of a WT. A method which can be used to estimate this parameter is found in [41].

Additionally, the behaviour of the CB system complements this control of the reactive power peaks. The influence of this protection system is shown in Fig. 13, in which the parameter $1/x_s = 2.5$ for this case. On the one hand, when the fault occurs (Zoom 1), the CB system actuates countering the peak, since it multiplies by zero the commanded reactive current. In fact, the

adjustment of the parameters of the CB system, as well as x_s , allows a flexible control of these peaks, which is not possible with the WECC system. On the other hand, when the fault is cleared (Zoom 2), the negative value of the peak is accentuated by the cancellation of the reactive current command signal. Indeed, the WECC model is unable to model this behaviour, and as shown in Fig. 13, the rise and fall are commanded by the control system, which results in uncontrolled peaks in transient periods. Real WT's reactive power responses do not show the peaks modelled by the WECC model, but they are highly similar to the IEC behaviour [32].

4.3 Complexity and simulation time

As explained in Section 1, IEC and WECC modelling approaches focus on different aspects. While the IEC centres on accuracy and better emulation of transient periods, the WECC guidelines focus on reducing the number of parameters and the simulation time. Since the greater flexibility of the IEC model has been clearly illustrated by the previous results, the authors also tested the advantages of the simplicity of the WECC model.

First, the number of parameters and Simulink blocks were calculated using the MATLAB command `sdiagnostics`. If blocks such as input or 'go to' blocks (which do not contribute to the complexity of the model) are disregarded, the IEC model is defined by ~ 100 parameters and 435 Simulink blocks. The WECC model is defined by ~ 75 parameters and 260 Simulink blocks. Thus, one of the objectives of the WECC model is achieved, since the definition and modelling of its model is simpler than the IEC approach.

Concerning the simulation time, which is highly related to the complexity of the model, the authors ran simulations of 5 s of a voltage dip of 500 ms of duration and 0.5 pu of depth. Two different tests were conducted with each modelling approach (IEC and WECC): (i) 500 simulations of one WT, (ii) 250 simulations of ten WTs. The simulations were carried out using the fixed-step solver `ode4` (Runge–Kutta) and with a step size of 1 ms. The computer used is equipped with an Intel(R) Core(TM) i7-4720HQ central processing unit, working at 2.60 GHz, 8 GB of random access memory, and running in a 64 bits operational system. Box plots are used to summarise the simulation duration results, see Fig. 14. It can be observed in both tests that the time used by the IEC model doubles the time of the WECC model. Hence, this constitutes an important limitation of the IEC model, which needs larger computational resources.

Regarding the extra accuracy provided by the IEC model, the cases, in which it is most important are the transient periods. However, most of the validation methods, and even the IEC validation method itself, disregard these transient periods [44], assuming the inability of the generic models when modelling certain behaviours. When the fault occurs, according to IEC 61400-27-1 [7], the mean absolute error and the maximum error should not be calculated during the first 140 ms. This is due to the limitation of replicating the DC-component of the generator flux by the model. Moreover, when the fault is cleared, the maximum error should not be calculated within the first 500 ms. During this period, the reactive power is affected by the transformer inrush, whereas the active power may be modified by aerodynamic and mechanical fluctuations. Thus, as shown in the simulations, most of the periods, in which the differences between the two international guidelines are larger are dismissed by this validation methodology. Hence, stakeholders should assess their particular needs in order to prioritise the simulation time or the accuracy.

5 Conclusions

This work has provided a better understanding of the generic Type 3 (DFIG) WT models under development by international organisations. In February 2015, the IEC published the Standard IEC 61400-27-1, and in January 2014, the WECC published the WECC Second Generation WT Models. Both of these documents define generic WT models, which can be adapted to any specific vendor model by adjusting a limited number of parameters.

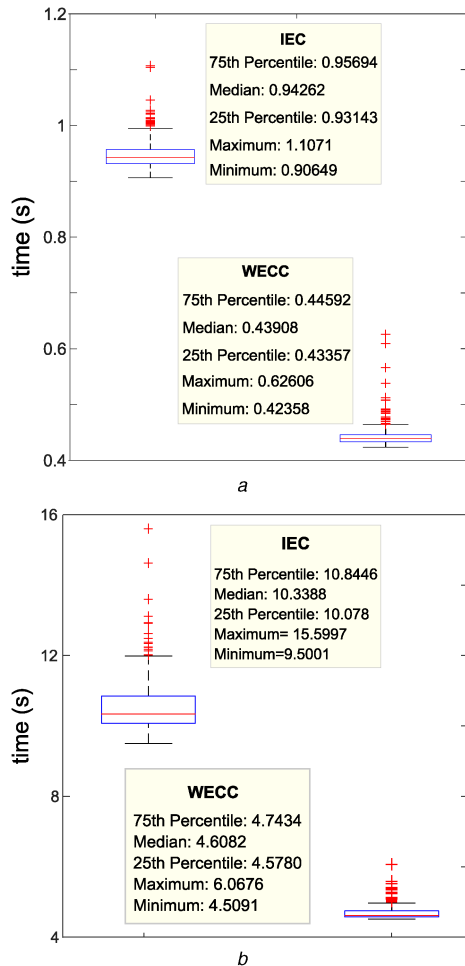


Fig. 14 Comparison of simulation times
(a) Boxplot of simulation times for test 1, (b) Boxplot of simulation times for test 2

Although both international guidelines were developed in conjunction, as they focus on different aspects (simplicity versus exact representation of faults), the implementations differ. Type 3 represents what is currently the most conventional technology, and this model is the most complex of the four types in both organisations. In this work, the generic Type 3 models, developed following the guidelines provided by both Committees, were implemented in MATLAB/Simulink, and adjusted in order to provide the most similar response. First, the general structure of both models is described, highlighting the main similarities and differences. Then, the systems that most differ between both modelling approaches are analysed. The active power control system is one of the most different models, with the IEC being more flexible in the modelling of fault and post-fault responses. Regarding the reactive power control, the main differences are a result of the different control logics of the models. The behaviour of the CLS is similar during the voltage dip. However, the IEC system includes more conditions when providing the maximum and minimum current. Finally, the generator system described by WECC is modelled by first-order filters and saturation blocks, while the IEC system is more complex and includes the dynamics of the electrical generator reactance, as well as the grid voltage coordination. However, the WECC model includes LVPL and active current management systems, providing some flexibility as well.

As a consequence, on the one hand, the generic IEC 61400-27-1 Type 3 model is more complex than the WECC model. It includes systems such as the active DTD in active power control, the CB protection system in the generator model and even a dynamic reactive power limiter control system, which result in a more accurate response when compared with the field response of real WTs, due to the higher transient response control. Moreover, the IEC approach represents the WT model in a more open manner,

without being linked to any specific software (such as GE PSLF™ and Siemens PTI PSS®E). On the other hand, the WECC model needs fewer parameters and blocks for its definition and modelling than the IEC model. This leads to the simulation time of the WECC model being approximately more than 50% smaller than that of the IEC model.

Finally, while the IEC model can adapt its response to that of the WECC by the adjustment of its parameters, conversely it is impossible for the WECC system to emulate certain behaviours. Nevertheless, the need to include specific systems such as that previously mentioned, has been rejected by the WECC committee, because they consider they do not significantly affect the behaviour of the WT response, and complicate the model unnecessarily. Additionally, most of the differences in the model response occur during the transient periods, which may be dismissed for some studies (e.g. the IEC validation methodology itself disregards some time windows during transient periods). Thus, as both committees decided to set a different focus, the stakeholders (researchers, WT manufacturers, DSOs, TSOs, ...) implementing these models should decide about their highest concern: accuracy or simplicity.

In summary, this paper has shown the differences between the generic Type 3 WT models developed by IEC and WECC, as well as the consequences of the different focus of each guideline. It has been shown that both these models can provide comparable responses of active and reactive powers, and hence, projects which have used different models can be coordinated to obtain similar results. However, depending on the study to be conducted, the more flexible control systems provided by the IEC model may be necessary. For cases that do not require modelling transient periods, the simplicity of the WECC model can be used in advance since lower computational resources are needed. Finally, the different focus of each entity constitutes a clear advantage for stakeholders, who can choose the model that best fits their needs.

6 Acknowledgments

This work was supported by the ‘Ministerio de Economía y Competitividad’ and European Union FEDER, which supported this work under project ENE2016-78214-C2-1-R. This work has received funding from the Agreement signed between the UCLM and the Council of Albacete to foster the Research in the Campus of Albacete

7 References

- [1] Basit, A., Hansen, A.D., Altin, M., *et al.*: ‘Wind power integration into the automatic generation control of power systems with large-scale wind power’, *J. Eng.*, 2014, **2014**, (10), pp. 538–545. Available at: <http://digital-library.theiet.org/content/journals/10.1049/joe.2014.0222>, accessed 21 February 2019
- [2] Hu, J., Huang, Y., Wang, D., *et al.*: ‘Modeling of grid-connected DFIG-based wind turbines for dc-link voltage stability analysis’, *IEEE Trans. Sustain. Energy*, 2015, **6**, (4), pp. 1325–1336
- [3] Prajapat, G.P., Senroy, N., Kar, I.N.: ‘Wind turbine structural modeling consideration for dynamic studies of DFIG based system’, *IEEE Trans. Sustain. Energy*, 2017, **8**, (4), pp. 1463–1472
- [4] Hu, Y.L., Wu, Y.K.: ‘Comparative analysis of generic and complex models of the type-3 wind turbine’. 2016 IEEE PES Asia-Pacific Power and Energy Engineering Conf. (APPEEC), Xi’an, China, 2016, pp. 392–396
- [5] Honrubia-Escribano, A., Jiménez-Buendía, F., Molina-García, A., *et al.*: ‘Analysis of wind turbine simulation models: assessment of simplified versus complete methodologies’. XVII Int. Symp. Electromagnetic Fields in Mechatronics, Electrical and Electronic Engineering, Valencia, Spain, 2015, p. 8
- [6] Aziz, A., Amanullah, M., Vinayagam, A., *et al.*: ‘Modelling and comparison of generic type 4 WTG with EMT type 4 WTG model’. 2015 Annual IEEE India Conf. (INDICON), New Delhi, India, 2015, pp. 1–6
- [7] International Electrotechnical Commission: ‘IEC 61400-27-1: electrical simulation models for wind power generation – wind turbines’, 2015
- [8] WECC REMTF: ‘WECC second generation of wind turbine models’ (WECC, USA, 2014)
- [9] WECC: ‘WECC first generation of wind turbine models’ (WECC, USA, 2010)
- [10] Sørensen, P.: ‘Introduction to IEC 61400-27. Electrical simulation models for wind power generation’. EERA Workshop on Generic Electric Models for Wind Power, Amsterdam, Netherlands, 2012
- [11] Honrubia-Escribano, A., Gómez-Lázaro, E., Viguera-Rodríguez, A., *et al.*: ‘Assessment of DFIG simplified model parameters using field test data’. IEEE Symp. Power Electronics & Machines for Wind Application, Denver, USA, 2012, pp. 1–7

- [12] Cristina-Vázquez-Hernández, T.T., Pradas, A.V.: 'JRC wind energy status report 2016 edition'. Market, technology and regulatory aspects of wind energy. JRC Science for policy report, 2017
- [13] Pourbeik, P.: 'Proposed changes to the WECC WT3 generic model for type 3 wind turbine generators' (Electric Power Research Institute, USA, 2014)
- [14] Behnke, M., Ellis, A., Kazachkov, Y., *et al.*: 'Development and validation of WECC variable speed wind turbine dynamic models for grid integration studies'. AWEA WindPower Conf., Los Angeles, USA, 2007, p. 5
- [15] Fortmann, J., Sørensen, P.: 'IEC work on modelling – generic model development. IEC 61400-27 – expected outcome', 2011
- [16] Sørensen, P., Andersen, B., Fortmann, J., *et al.*: 'Overview, status and outline of the new IEC 61400-27 – electrical simulation models for wind power generation'. Tenth Int. Workshop on Large-Scale Integration of Wind Power into Power Systems as well as on Transmission Networks for Offshore Wind Power Farms, Aarhus, Denmark, 2011, p. 6
- [17] Sørensen, P., Andersen, B., Bech, J., *et al.*: 'Progress in IEC 61400 – 27. Electrical simulation models for wind power generation'. 11th Int. Workshop on Large-Scale Integration of Wind Power into Power Systems as well as on Transmission Networks for Offshore Wind Power Farms, Lisbon, Portugal, 2012, p. 7
- [18] Asmine, M., Brochu, J., Fortmann, J., *et al.*: 'Model validation for wind turbine generator models', *IEEE Trans. Power Syst.*, 2011, **26**, (3), pp. 1769–1782
- [19] Keung, P.K., Kazachkov, Y., Senthil, J.: 'Generic models of wind turbines for power system stability studies'. IET Conf. Proc., London, UK, 2009, pp. 128–128(1). Available at: <http://digital-library.theiet.org/content/conferences/10.1049/cp.2009.1785>, accessed 21 February 2019
- [20] Ellis, A., Kazachkov, Y., Muljadi, E., *et al.*: 'Description and technical specifications for generic WTG models – a status report'. IEEE/PES Power Systems Conf. Exposition (PSC), Phoenix, USA, 2011, pp. 1–8
- [21] Pourbeik, P.: 'Proposed changes to the WECC WT3 generic model for type 3 wind turbine generators' (Electric Power Research Institute, USA, 2012)
- [22] Pourbeik, P., Ellis, A., Sanchez-Gasca, J., *et al.*: 'Generic stability models for types 3 & 4 wind turbine generators for WECC'. IEEE Power and Energy Society General Meeting, Vancouver, Canada, 2013, pp. 1–5
- [23] Sørensen, P., Andresen, B., Fortmann, J., *et al.*: 'Modular structure of wind turbine models in IEC 61400-27-1'. IEEE Power and Energy Society General Meeting, Vancouver, Canada, 2013, pp. 1–5
- [24] Fortmann, J., Engelhardt, S., Kretschmann, J., *et al.*: 'New generic model of DFG-based wind turbines for RMS-type simulation', *IEEE Trans. Energy Convers.*, 2014, **29**, (1), pp. 110–118
- [25] Sørensen, P., Fortmann, J., Jiménez-Buendía, F., *et al.*: 'Final draft international standard IEC 61400-27-1. Electrical simulation models of wind turbines'. 13th Wind Integration Workshop, Berlin, Germany, 2014, p. 5
- [26] Honrubia-Escribano, A., Gómez-Lázaro, E., Fortmann, J., *et al.*: 'Generic dynamic wind turbine models for power system stability analysis: a comprehensive review', *Renew. Sustain. Energy Rev.*, 2018, **81**, pp. 1939–1952
- [27] Lorenzo-Bonache, A., Honrubia-Escribano, A., Jiménez-Buendía, F., *et al.*: 'Generic type 3 wind turbine model based on IEC 61400-27-1: parameter analysis and transient response under voltage dips', *Energies*, 2017, **10**, (9), p. 23
- [28] Lorenzo-Bonache, A., Villena-Ruiz, R., Honrubia-Escribano, A., *et al.*: 'Operation of active and reactive control systems of a generic Type 3 WT model'. IEEE Int. Conf. Compatibility, Power Electronics and Power Engineering, Cádiz, Spain, 2017
- [29] Ellis, A., Pourbeik, P., Sanchez-Gasca, J.J., *et al.*: 'Generic wind turbine generator models for WECC – a second status report'. IEEE Power and Energy Society General Meeting, Denver, USA, 2015, pp. 1–5
- [30] Richwine, M.P., Sanchez-Gasca, J.J., Miller, N.W.: 'Validation of a second generation type 3 generic wind model'. IEEE Power Energy Society General Meeting, Washington DC, USA, 2014, pp. 1–4
- [31] Honrubia-Escribano, A., Jiménez-Buendía, F., Gómez-Lázaro, E., *et al.*: 'Validation of generic models for variable speed operation wind turbines following the recent guidelines issued by IEC 61400-27', *Energies*, 2016, **9**
- [32] Honrubia-Escribano, A., Jiménez-Buendía, F., Gomez-Lázaro, E., *et al.*: 'Field validation of a standard type 3 wind turbine model for power system stability, according to the requirements imposed by IEC 61400-27-1', *IEEE Trans. Energy Convers.*, 2017, **PP**, (99), p. 1
- [33] Lorenzo-Bonache, A., Honrubia-Escribano, A., Jimenez, F., *et al.*: 'Field validation of generic type 4 wind turbine models based on IEC and WECC guidelines', *IEEE Trans. Energy Convers.*, 2018, p. 1
- [34] Göksu, Ö., Altin, M., Fortmann, J., *et al.*: 'Field validation of IEC 61400-27-1 wind generation type 3 model with plant power factor controller', *IEEE Trans. Energy Convers.*, 2016, **31**, (99), pp. 1170–1178
- [35] Pourbeik, P., Etsel, N., Wang, S.: 'Model validation of large wind power plants through field testing', *IEEE Trans. Sustain. Energy*, 2017, **9**, pp. 1212–1219
- [36] Göksu, Ö., Sørensen, P., Morales, A., *et al.*: 'Compatibility of IEC 61400-27-1 Ed 1 and WECC 2nd generation wind turbine models'. 15th Wind Integration Workshop, Vienna, Austria, 2016
- [37] Lorenzo-Bonache, A., Villena-Ruiz, R., Honrubia-Escribano, A., *et al.*: 'Comparison of a standard type 3B WT model with a commercial build-in model'. IEEE Int. Electric Machines & Drives Conf., Miami, USA, 2017
- [38] WECC REMTF: 'WECC second generation of wind turbines models guidelines' (WECC, USA, 2014)
- [39] Pourbeik, P., Sánchez-Gasca, J.J., Senthil, J., *et al.*: 'Value and limitations of the positive sequence generic models of renewable energy systems', This is a brief white-paper prepared by an Ad hoc group within the WECC Renewable Energy Modeling Task Force, 2015
- [40] Pourbeik, P.: 'Model user guide for generic renewable energy system models' (Electric Power Research Institute, USA, 2015)
- [41] Fortmann, J.: 'Modeling of wind turbines with doubly fed generator system' (Department for Electrical Power Systems, University of Duisburg-Essen, 2014)
- [42] Jiménez-Buendía, F., Barrasa-Gordo, B.: 'Generic simplified simulation model for DFIG with active crowbar'. 11th Wind Integration Workshop, Lisbon, Portugal, 2012, p. 6
- [43] WECC REMTF: 'WECC wind power plant dynamic modeling guidelines' (WECC, USA, 2014)
- [44] Li, Q., He, J., Qin, S., *et al.*: 'Wind turbine model validation based on state interval and error calculation', *J. Eng.*, 2017, **2017**, pp. 762–767. Available at: <http://digital-library.theiet.org/content/journals/10.1049/joe.2017.0434>, accessed 21 February 2019